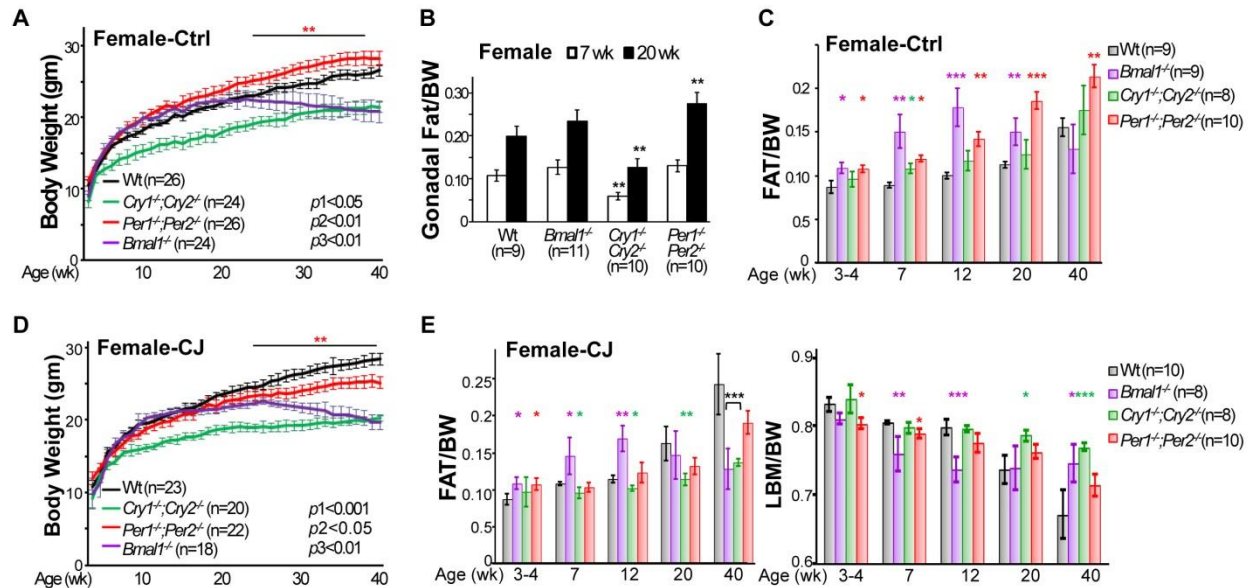


## Supplemental Information

### Supplemental Figures and Legends



**Figure S1. Body weight and composition phenotypes of female mice (Related to Figure 1).**

A. Body weight of control (Ctrl) female mice kept in 24hr LD cycles from 4-40 weeks of age ( $p_1$ : Wt vs. *Cry*-mutants from 3-40 weeks of age,  $p_2$ : Wt vs. *Per*-mutants from 15-35 weeks of age, and  $p_3$ : Wt vs. *Bmal1<sup>-/-</sup>* mice from 12-40 weeks of age). B. Ratios of gonadal fat mass vs. body weight (BW) of female mice kept in 24hr LD cycles at 7 and 20 weeks of age ( $\pm$ SEM). C. Fat composition of female mice kept in stable 24hr LD cycles between 4-40 weeks of age ( $\pm$ SEM). D. Body weight of chronically jet-lagged (CJ) female mice from 4-40 weeks of age ( $p_1$ : Wt vs. *Cry*-mutants from 3-40 weeks of age,  $p_2$ : Wt vs. *Per*-mutants between 28-40 weeks of age, and  $p_3$ : Wt vs. *Bmal1<sup>-/-</sup>* mice from 25 to 40 weeks

of age). E. Fat (left panel) and lean body mass (LBM) (right panel) compositions of female mice under chronic jet-lag condition from 4-40 weeks of age ( $\pm$ SEM). \* $p < 0.05$ , \*\* $p < 0.01$  and \*\*\* $p < 0.001$ , Student  $t$  test.

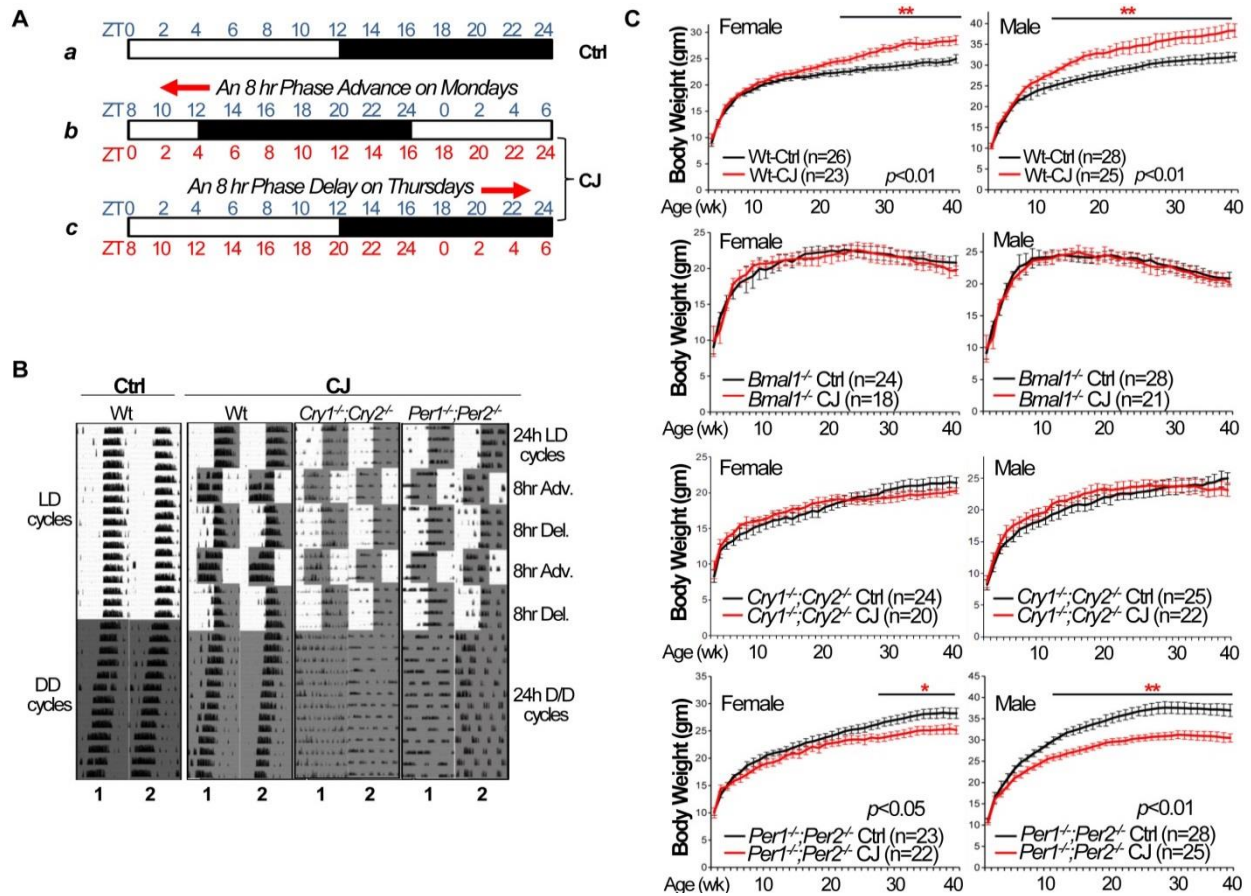


**Figure S2. The effects of chronic jet-lag on mouse volunteer locomotor activity and body weight (Related to Figure 1).**

A. A schematic representation of chronic jet-lag (CJ) protocol. Control (Ctrl) mice were maintained in steady 24hr LD cycles (a). Transferring mice from condition (a) to (b) resulted in an 8hr phase advance on the day of transfer, while transferring mice from (b) to (c) induced an 8hr phase delay on the day of the transfer. Numbers on the top of the bar (blue) in (b) and (c) indicate ZT times in the new time zone. Numbers below the bar

(red) indicate the ZT times in old time zone. Arrows indicate the directions of phase shifts. Mice are transferred from condition *a* to *b* on each Monday and then *b* to *a* on each Thursday. B. Representative locomotor activity records of male Wt, *Cry1*<sup>-/-</sup>;*Cry2*<sup>-/-</sup> and *Per1*<sup>-/-</sup>;*Per2*<sup>-/-</sup> mice in steady 24hr LD cycles, under jet-lag conditions and in 24hr DD cycles (Adv: phase advance. Del: phase delay). C. Chronic jet-lag increased average body weight in both male and female Wt mice, had no significant effect on *Bmal1*<sup>-/-</sup> and *Cry1*<sup>-/-</sup>;*Cry2*<sup>-/-</sup> mice, but decreased body weight of both male and female *Per1*<sup>-/-</sup>;*Per2*<sup>-/-</sup> mice. \**p*<0.05 and \*\**p* < 0.01, student *t* test.

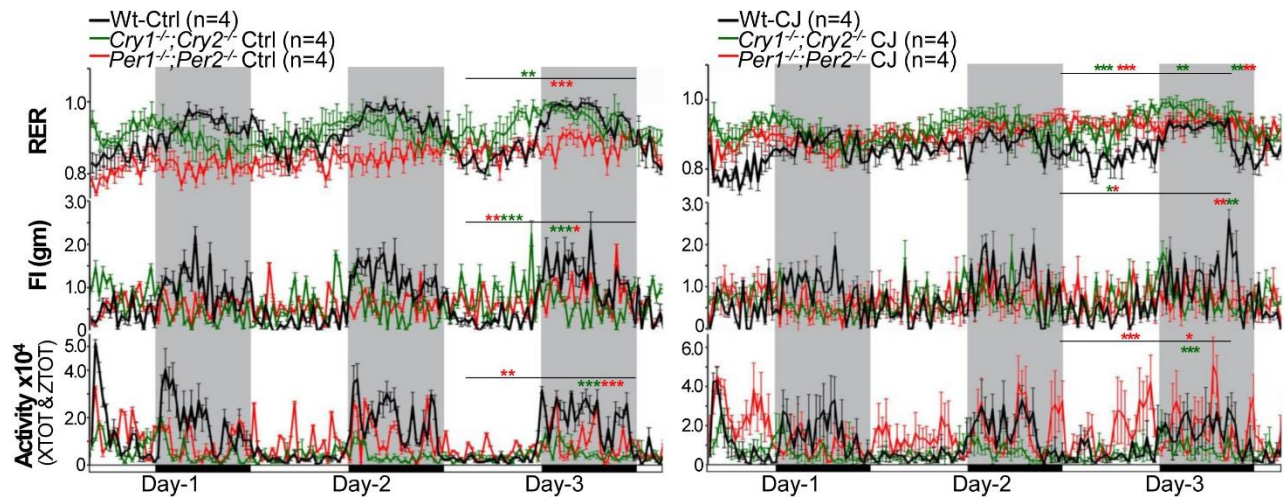


**Figure S3. Circadian disruption differentially disrupts energy homeostasis in different mouse models (Related to Figure 2).**

Circadian profiles of respiration exchanging rate (RER), food-intake (FI) and physical activity of control (left panel) and chronically jet-lagged (right panel) male Wt, *Cry1*<sup>-/-</sup>;*Cry2*<sup>-/-</sup> and *Per1*<sup>-/-</sup>;*Per2*<sup>-/-</sup> mice over 3 consecutive 24hr LD cycles as measured by CLAMS. \* Compare to Wt mice, \*\**p* < 0.01 and \*\*\**p* < 0.001, Student *t* test.

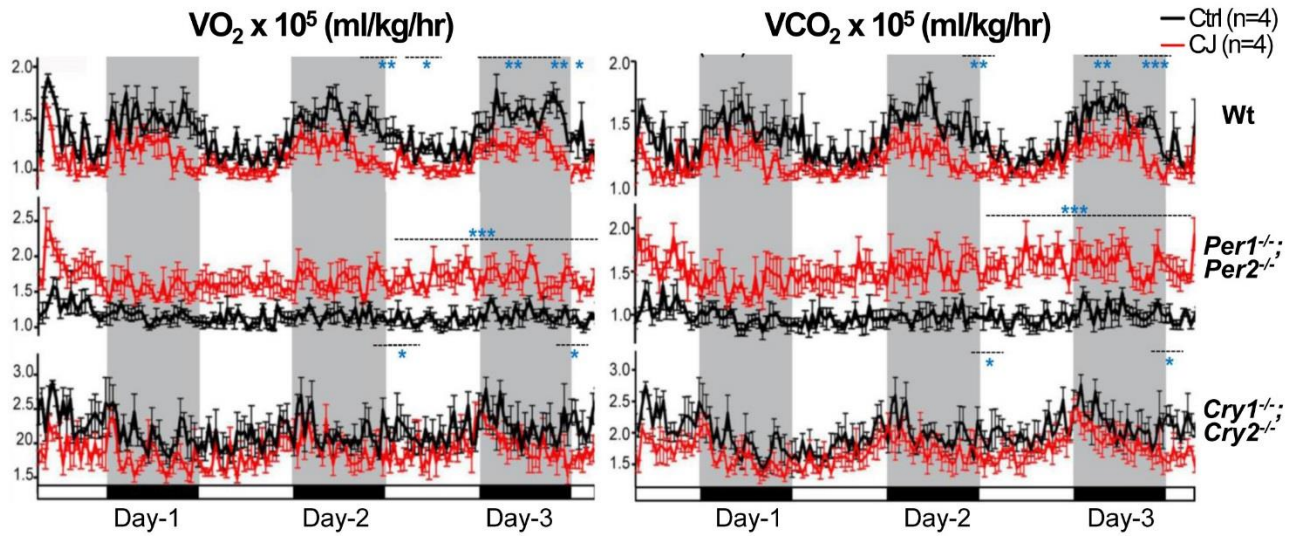


**Figure S4. Circadian disruption differentially shifts energy expenditure in different mouse models (Related to Figure 2).**

Changes in oxygen consumption ( $VO_2$ ) (left panel) and carbon dioxide production ( $VCO_2$ ) (right panel) induced by chronic jet-lag in male Wt,  $Cry1^{-/-};Cry2^{-/-}$  and  $Per1^{-/-};Per2^{-/-}$  mice as measured by CLAMS over 3 consecutive 24hr LD cycles. \* Compare to control mice of the same genotype. \*  $p < 0.05$ , \*\*  $p < 0.01$  and \*\*\*  $p < 0.001$ , student  $t$  test.

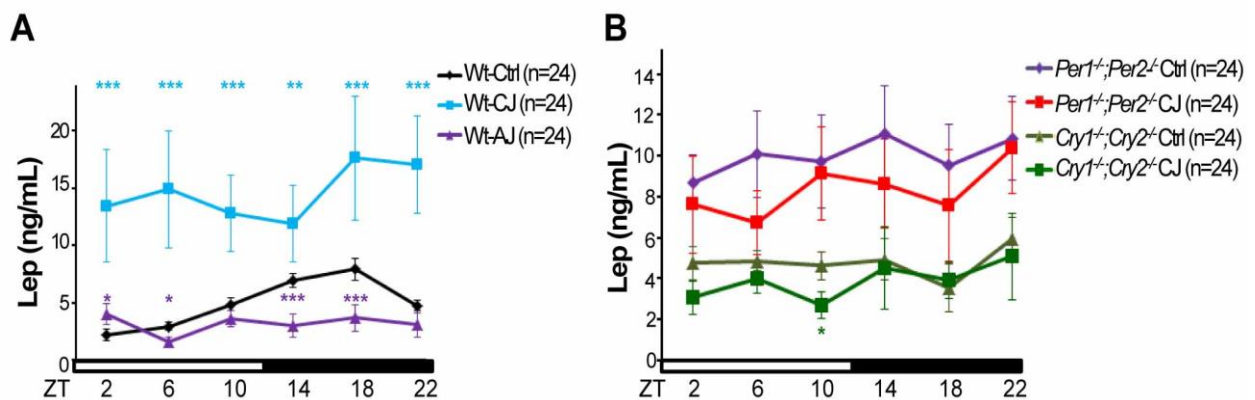


**Figure S5. Circadian disruption abolishes homeostasis of plasma Leptin (Related to Figure 3).**

A. Changes in plasma levels of Leptin (Lep) in acute jet-lagged (AJ) and chronically jet-lagged male Wt mice. B. Plasma levels of Leptin in control and chronically jet-lagged male *Cry1<sup>-/-</sup>;Cry2<sup>-/-</sup>* and *Per1<sup>-/-</sup>;Per2<sup>-/-</sup>* mice. \* Compare to control mice of the same genotype at the same time. \**p* < 0.05, \*\**p* < 0.01 and \*\*\**p* < 0.001, student *t* test.

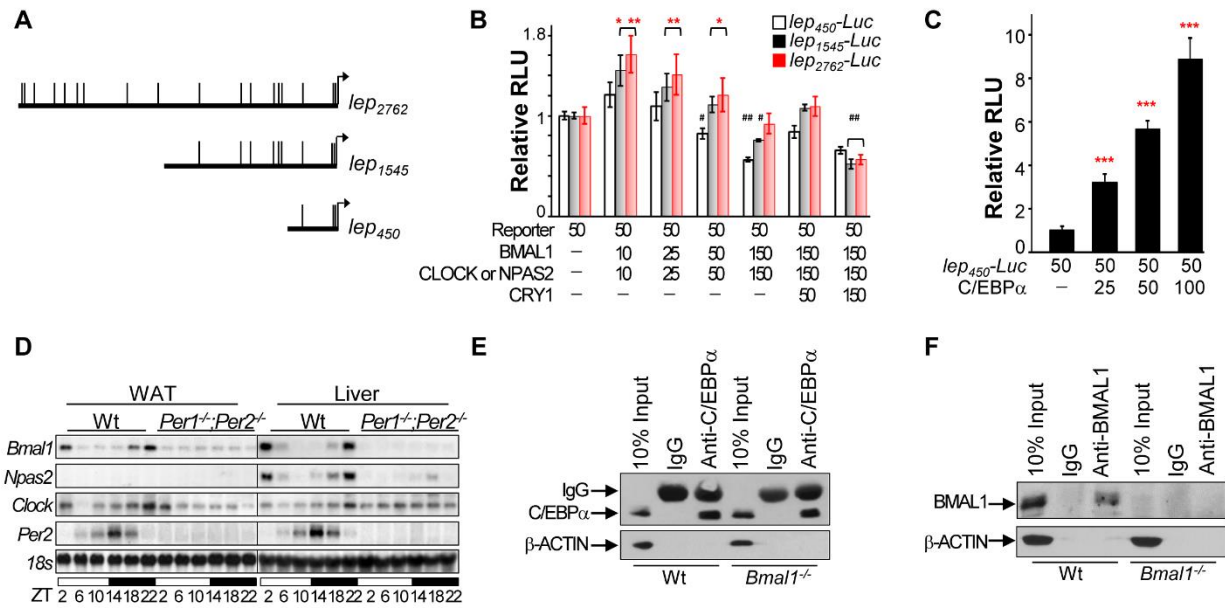


**Figure S6. The molecular clock controls *leptin* transcription (Related to Figures 4 and 5).**

A. A schematic illustration of the positions of consensus E-boxes in the *leptin<sub>2762</sub>-Luc*, *leptin<sub>1545</sub>-Luc* and *leptin<sub>450</sub>-Luc* reporters described in the main text. B. The dual role of heterodimer in controlling the *lep-Luc* reporter activity is affected by the length of *leptin* promoter: the *lep<sub>2762</sub>-Luc* reporter was most sensitive to the stimulatory effect of the heterodimer at a low concentration, the *lep<sub>1545</sub>-Luc* displayed a moderate response to changes in the level of the heterodimer, while the *lep<sub>450</sub>-Luc* reporter was most efficiently inhibited by a high expression level of the heterodimer ( $\pm$ SEM, \*: stimulation and #: suppression; \*/#*p* < 0.05, \*\*/##*p* < 0.01 and \*\*\**p* < 0.001, student *t* test). C. Co-transfection

assays show that C/EBP $\alpha$  is a strong activator of the *leptin* promoter ( $\pm$ SEM, \*\*\* $p < 0.001$ , student *t* test). D. Northern blotting show tissue-specific expression of *Npas2*. All clock genes studied are expressed in both WAT and livers in Wt mice, except *Npas2*, which is only expressed in Wt livers but not WAT. E-F. Representative IP/Western images for validating the efficiencies of anti-C/EBP $\alpha$  (E) and anti-BMAL1 (F) antibodies in immunoprecipitation using nuclear extracts prepared from WAT of Wt and *Bmal1*<sup>-/-</sup> mice at ZT2.

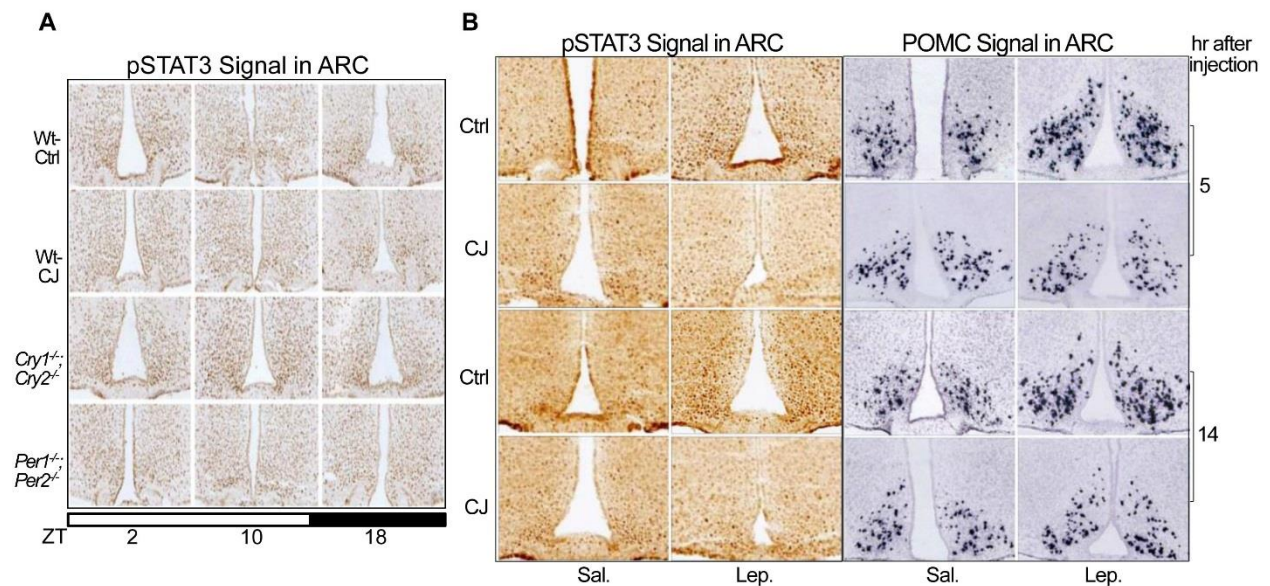


**Figure S7. Circadian disruption abolishes the homeostasis of ARC neuron activity (Related to Figure 6).**

A. Representative immunohistochemistry (IHC) images of pSTAT3 signals in the ARC of control and jet-lagged Wt mice and *Cry* -and *Per*-mutant mice at ZT2, 10 and 18. B. Representative IHC signals of pSTAT3 (left) and *in situ* signals of POMC (right) in the ARC of Wt control and jet-lagged mice at 5 and 14hr after a single exogenous Leptin administration.

## Supplemental Experimental Procedures

### Mouse Models

The Tyrc-Brd allele in C57BL/6J-Tyr inbred strain of *Per1*<sup>-/-</sup> (Zheng et al., 2001) and *Per2*<sup>-/-</sup> mice [Fig. S3A-B in (Fu et al., 2002)] were bred out by crossing serially with C57BL/6J wild-type (Wt) mice from the Jackson Laboratory for 8 generations. The resulting C57BL/6J inbred *Per1*<sup>-/-</sup> and *Per2*<sup>-/-</sup> mice were mated to generating *Per1*<sup>-/-</sup>;*Per2*<sup>-/-</sup> mice. C57BL/6J inbred *Bmal1*<sup>+/-</sup> and *Cry1*<sup>-/-</sup>;*Cry2*<sup>+/-</sup> mice were kind gifts from Dr. Christopher Bradfield (Bunger et al., 2000) and Dr. Aziz Sancar (Selby et al., 2000), respectively. C57BL/6J inbred *Bmal1*<sup>fl/fl</sup> mice were purchased from the Jackson Laboratory and crossed to C57BL/6J inbred *Ap2-cre* transgenic mice to generate *Ap2*<sup>Cre</sup>;*Bmal1*<sup>fl/fl</sup> mice. All C57BL/6J inbred mouse models described were backcrossed to the C57BL/6J inbred Wt mice from the Jackson Laboratory for 3 additional generations before used for generating *Bmal1*<sup>-/-</sup>, *Per1*<sup>-/-</sup>;*Per2*<sup>-/-</sup>, *Cry1*<sup>-/-</sup>;*Cry2*<sup>-/-</sup> and *Ap2*<sup>Cre</sup>;*Bmal1*<sup>fl/fl</sup> mice used in the study. *Per1*<sup>+/+</sup>;*Per2*<sup>+/+</sup>, *Bmal1*<sup>+/+</sup> and *Cry1*<sup>+/+</sup>;*Cry2*<sup>+/+</sup> littermates from the last breeding cycle described above were crossed to generate Wt control mice for all experiments described. Female mice were only used in body weight and composition studies. All other experiments described used male mice.

### Animal Maintenance

Mice were housed as 2-5 per cage in standard pathogen-free conditions and fed ad libitum with a standard mouse chow (Teklad Roden #2920X, 19% protein and 6% fat) and water in mouse rooms maintained in steady 12hr light/12hr dark cycles (24hr LD cycles)

with the temperature at 23°C to 25°C, humidity between 50%–70%, air-flow rate of 15 exchanges. Jet-lagged mice are maintained in the same condition, except that they were transferred between two mouse rooms different only at the time of light onset for 8 hrs (Room 1: 6:00am to 6:00pm light/6:00pm to 6:00am dark, and Room 2: 10:00am to 10:00pm dark/10:00pm to 10:00am light) (Fig.S2A). Husbandry and vet inspection were performed in room 1 only (weekly mouse cage change between 9:00 am to 11:00 am on Thursdays and vet inspection before 10:00am on Mondays and Thursdays). Body weight and composition of control and jet-lagged mice were recorded on Thursdays between 11:00am to 12:30 pm after cage changes (ZT5-6.5). Mice treated by acute jet-lag were at 12-16 weeks of age and transferred once from room 1 to 2 and then returned to room 1. The time of mouse transfer occurs between 9:30am to 10:00am, leading to an 8hr phase advance from room 1 to 2 on Monday (light off at ZT4 instead of ZT12 for jet-lagged mice on the day of transfer) and an 8hr phase delay from room 2 to 1 on Thursday (light off at ZT20 instead of ZT12 for jet-lagged mice on the day of transfer) (Fig. S2A). Chronically jet-lagged (CJ) mice were transferred between room 1 and 2 as described from 4 to 40 weeks of age.

## **CLAMS**

Energy homeostasis of mice was studied by a Comprehensive Lab Animal Monitoring System (CLAMS, Columbia Instruments) kept in a mouse room under the exactly same light/dark, temperature, humidity and ventilation conditions as described above. The CLAMS simultaneously measures food intake, physical activities and energy expenditure of 12 single-housed mice for 3 consecutive days. Two independent CLAMS analyses



each studied 2 control and chronic jet-lagged male *Wt*, *Cry1<sup>-/-</sup>;Cry2<sup>-/-</sup>* and *Per1<sup>-/-</sup>;Per2<sup>-/-</sup>* male mice at 16-18 weeks of age on the second day after all jet-lagged mice completed their last cycle of jet-lag. Mice were loaded on metabolic cages between 9:30 am to 10:00 am on day 1 of each CLAMS study and fed ad libitum with the standard mouse chow and water. The CLAMS measures food-intake as changes in the weight of food-supplied to individual mice, physical activity as XYZ laser beam interruption, energy expenditure as the rate of oxygen consumption ( $VO_2/hr$ ) and carbon dioxide production ( $VCO_2/hr$ ), and respiratory exchange ratio (RER) every 20 min during the 3-day period (Kokkotou et al., 2005). Energy expenditure was calculated as the milliliter of  $O_2$  or  $CO_2$  produced from one kilogram of LBM per hour (ml/kg/hr). LBM is the average LBM measured at the start and end of each CLAMS analysis.

### **Body Composition Studies**

Fat and lean body mass (LBM) of male and female mice were measured at 3, 7, 12, 20 and 40 weeks of age using an EchoMRI Whole Body Composition Analyzer (Echo Medical Systems). Body composition was calculated as the ratio of total body fat or lean body mass to body weight.

### **Behavioral Analysis**

Volunteer wheel running activity of male *Wt*, *Cry1<sup>-/-</sup>;Cry2<sup>-/-</sup>* and *Per1<sup>-/-</sup>;Per2<sup>-/-</sup>* mice of 10-12 weeks of age was studied in light-proof circadian chambers. Mice fed ad libitum with a standard mouse chow (Teklad Roden #2920X) and water, and were entrained in stable 24 LD cycles prior to data acquisition. Their volunteer locomotor activities in 24hr LD or

DD cycles, or in response to weekly forward and backward 8hr shifts of light cues were monitored in 5-min intervals using an online PC computer connected to the MiniMitter Running Wheel Activity System via magnetic switches and analyzed by the VitalView Data Acquisition System and ActiView 1.3 Software (MiniMitter Company, Inc. Sunriver, OR, USA) (Greenwood et al., 2012).

### **Intraperitoneal injection of Leptin**

Single-housed male Wt and *Per1*<sup>-/-</sup>;*Per2*<sup>-/-</sup> mice at 10-14 weeks of age were entrained in circadian chambers for two weeks before being used for a single intraperitoneal injection of saline or recombinant mouse Leptin (National Hormone & Peptide Program, CA) at a dose of 1.25 µg per gm body weight at ZT12. Jet-lagged Wt mice were treated with chronic jet-lag from 4-5 weeks of age before the experiment. Body weight of mice and the total amount of food in each mouse cage were recorded prior to and at 24hr after injection. The changes in body weight and the amount of food intake of each mouse over a 24hr period after injection were used for analyzing mouse response to exogenous Leptin administration.

Additional groups of Wt control and jet-lagged mice (n=3 each group) were sacrificed at 5hr (ZT17) or 14hr (ZT2) after a single intraperitoneal injection of saline or recombinant mouse Leptin by cervical dislocation. Serum and brains were isolated from these mice and used for immunohistochemistry (IHC), *in situ*, and ELISA analyses.

### **Mouse Tissue and Serum Collection**

Control mice were single-housed, entrained in 24hr LD cycles for 2-3 weeks in a circadian chamber before sacrificed by cervical dislocation at 12-16 weeks of age without disruption of mouse behavioral rhythm at ZT2, 6, 10, 14, 18 or 22, or first being entrained in 24hr LD cycles in a circadian chamber for two weeks and then switched to 24hr DD cycles for 24 hours before collecting tissues and serum at CT2, 6, 10, 14, 18, and 22. Mice used for studying plasma Leptin under fasting condition were first entrained in the chamber for two weeks. Food was then depleted from ZT2 to ZT22 on the day of blood collection. White adipose tissues (WAT), brain and blood were collected from mice in less than 1 minute after cervical dislocation. Samples from acute jet-lagged mice were collected on the second day after completing one cycle of forward and backward jet-lag (Friday) at ZT2, 6, 10, 14, 18 or 22. Samples from chronic jet-lagged mice were collected on the second day (Friday) after completing the last cycle of jet-lag at 12-16 weeks of age. Blood samples were collected by cardiac puncture and processed for serum isolation in 5-10 min after blood collection and then stored at -80°C until further analysis. Adipose tissues isolated from each mouse were evenly divided into two eppendorf tubes, snap-frozen in liquid nitrogen, and then immediately homogenized in trizol for extracting WAT RNA for Northern blot analysis or in 1x SDS-gel sample buffer to prepare total protein extracts for Western blot analysis. Brain samples were immediately processed for *in situ* and immunohistochemistry analysis. For collecting WAT for ChIP, about 3 to 6 grams of WAT obtained from 3 to 4 mice at the same time were pooled and immediately used for preparing nuclear extracts.

## **Western Blotting**

Protein expression was studied using total WAT protein or nuclear extracts following the standard procedure of Western blotting using anti-C/EBP $\alpha$  (Santa Cruz), BMAL1 and mouse Leptin (Abcam),  $\beta$ -Actin (Sigma), and PER2 and CRY1 antibodies (Lee et al., 2001).

### **Chromatin immunoprecipitation (ChIP)**

**Nuclear extracts preparation:** Freshly isolated WAT from control and jet-lagged male Wt mice or *Ap2<sup>cre</sup>;Bmal1<sup>fl/fl</sup>* mice of 12-16 weeks of age at ZT2, 10 or 18 were immediately cut into small pieces in 10mL 1X PBS-1mM PMSF at room temperature (RT) before adding formaldehyde to a final concentration of 1% for crosslinking. After incubating the mixture for 8 min at 25°C with shaking, the crosslinking reaction was stopped by the addition of 500  $\mu$ L of 2.5 M glycine and continuing incubation at RT for another 5 minutes with shaking. The WAT fragments were collected into a pre-chilled tubes, washed three times with 10 mL of ice-cold 1XPBS-1mM PMSF, and then homogenized using a dounce homogenizer on ice in a cold room in 15 mL of ice-cold homogenization buffer containing 10mM EDTA (pH 8.0), 10% glycerol, 0.5% Igepal (NP-40), 0.25% Triton-X-100, 1X complete protease inhibitor cocktail (Roche), and 1mM PMSF. The homogenates were transferred into a pre-chilled 50 ml centrifuge tube and spun at 2000 rpm for 10 minutes at 4°C. Supernatant containing fat floating on the top was removed and the pellet was re-suspended and washed twice using 5 mL of 1X PBS-1mM PMSF at 4°C by vigorous shaking for 10 minutes in a cold room before centrifugation at 2000 rpm for 5 minutes at 4°C. Nuclear pellet was then re-suspended in 500  $\mu$ L of sonication buffer containing 0.1M NaCl, 20mM HEPES pH7.5, 1.5mM EDTA pH8, 0.01%

Triton-X-100, 3mM Sodium beta-glycerophosphate, 1mM DTT, 1X complete protease inhibitor cocktail (Roche) and 1mM PMSF, and sonicated 3 times for 10 sec each on ice using a Branson Sonifier 150 sonicator at power level 3. Nuclear extracts were then collected by centrifugation at 10,000 rpm for 5 minutes at 4°C. After determining the size of chromatin fragments by electrophoresis and protein concentration by Bradford assay, the nuclear extracts were snap-frozen and stored in -80°C until further use.

***Immunoprecipitation and DNA extraction:*** Approximately 200 µg of nuclear extracts were diluted 10X using the sonication buffer and incubated for 1h at 4°C on a rotating wheel with 50 µL of protein G sepharose beads (GE Healthcare) pre-washed once with 1XPBS and once with sonication buffer for BMAL1 IP or 50 µL of Rabbit Ig IP beads (Rockland) pre-washed once with the sonication buffer for C/EBP $\alpha$  IP. After preclear, the lysates were incubated with either 1 µg of antibody or appropriate control IgG for 1 hour at 4°C with rotating [A guinea pig IgG (MBL International) was used as a control for the anti-BMAL1 antibody (Lee et al., 2001) and a rabbit IgG (Santa Cruz) was used as a control IgG for the anti-C/EBP $\alpha$  antibody (Santa Cruz)], and then mixed with 50 µL of protein G sepharose beads pre-blocked with 1 mL of 5mg/mL Protease Free BSA Fraction V Immunoglobulin (Rockland) for 30 minutes with shaking at RT for BMAL1 IP mixture, or 50 µL Rabbit Ig IP beads pre-washed once with ice-cold sonication buffer for C/EBP $\alpha$  IP mixtures. The IP reactions were first incubated overnight at 4°C with rotating, and then washed twice with a low salt washing buffer containing 10 mM Tris-HCl (pH 7.5), 150 mM NaCl, 1 mM EDTA (pH 8.0), 1% Triton-X-100, 0.1% Sodium-deoxycholate and 1mM PMSF, twice with a high salt washing buffer containing 20 mM Tris-HCl (pH 7.5), 500 mM NaCl, 2 mM EDTA (pH 8.0), 1% Triton X-100 and 1 mM

PMSF), twice with the LiCl wash buffer containing 20 mM Tris-HCl (pH 7.5), 250 mM LiCl, 2 mM EDTA (pH8.0), 0.5% Igepal CA-630, 1% sodium-deoxycholate and 1 mM PMSF, and twice with a buffer containing 2mM Tris-HCl (pH 7.5), 0.5 mM EDTA (pH 8.0) and 1mM PMSF for BMAL1 IP, or 6 times with sonication buffer for C/EBP $\alpha$  IP. Immunoprecipitated DNA fragments were then repeatedly eluted twice by incubating DNA-bead mixture with 50  $\mu$ L of a buffer containing 20 mM Tris-HCl (pH 7.5), 5 mM EDTA (pH 8.0) and 0.5% SDS in a 65°C shaking water bath for 10 minutes and then spun at 5000 rpm for 2 min at RT to collect DNA-containing supernatants. The eluted DNA of the same IP was first combined and then treated with reverse crosslinking at 65°C overnight with shaking, followed by RNaseA digestion (10  $\mu$ g/sample) for 1 hour at 37°C and then Proteinase K digestion (160  $\mu$ g/sample) for 1 hour at 55°C before purified by phenol/chloroform extraction. For input DNA, approximately 200  $\mu$ g of nuclear extracts were diluted 10X using the sonication buffer, boiled for 5 min and then treated with reverse crosslinking, RNase A digestion and Proteinase K digestion as described above before purification by phenol/chloroform extraction.

***qPCR to detect ChIP signals:*** The concentration and quality of DNA obtained from each ChIP reaction were determined by nano-drop. A dilution curve was performed on input and IP DNA to determine the optimal concentration for qPCR analysis. BMAL1 IP DNA was diluted 10X, C/EBP $\alpha$  IP DNA was diluted 15X, and 10% input DNA obtained from 200  $\mu$ g of nuclear extracts as described above was further diluted 10X and 15X as controls in qPCR analysis of BMAL1 and C/EBP $\alpha$  ChIP signals, respectively. The ChIP signals were studied by qPCR using a Roche LightCycler 480 Real-Time PCR system, PerfeCTa SYBR Green FastMix (Quanta BioSciences) and primers 5'

cctagaatggagcactagg 3' (forward) and 5' ccttaccttgacagctgc 3' (reverse) flanking the E-box1-2/CEBP $\alpha$  motif in *leptin* promoter, 5' ggttctgaggatgatgg 3' (forward) and 5' acctcagctagtgtgtaagg 3' (reverse) flanking the E-boxes 7 and 8 in the *leptin* promoter, 5' gtttcctttcacagtagcc 3' (forward) and 5' tagactgacattccctgg 3' (reverse) flanking the E-box 3 in *Per1* promoter, and 5' gtaattccacaggctgc 3' (forward) and 5' gttccgtgctatgatgc 3' (reverse) flanking the CEBP $\alpha$ -binding site in the *dhfr* promoter. Non-specific primers 5' ctgtacctgggggttcattcatt 3' (forward) and 5' cagtaagccgttcactctcaca 3' (reverse) correspondent to an untranslated region that does not contain an E-box or a C/EBP $\alpha$  binding site in mouse chromatin 13 were also used as negative controls. These primers did not detect any signal from any CHIP reactions in our experiments. The BMAL1 and C/EBP $\alpha$  binding to the promoters of genes studied were presented as the ratios of BMAL1 or C/EBP $\alpha$  CHIP signals verses their correspondent IgG CHIP signals.

### **Supplemental References**

Bunger, M.K., Wilsbacher, L.D., Moran, S.M., Clendenin, C., Radcliffe, L.A., Hogenesch, J.B., Simon, M.C., Takahashi, J.S., and Bradfield, C.A. (2000). Mop3 is an essential component of the master circadian pacemaker in mammals. *Cell* 103, 1009-1017.

Fu, L., Pelicano, H., Liu, J., Huang, P., and Lee, C. (2002). The circadian gene *Period2* plays an important role in tumor suppression and DNA damage response in vivo. *Cell* 111, 41-50.

Greenwood, B.N., Loughridge, A.B., Sadaoui, N., Christianson, J.P., and Fleshner, M. (2012). The protective effects of voluntary exercise against the behavioral consequences

of uncontrollable stress persist despite an increase in anxiety following forced cessation of exercise. *Behavioural brain research* 233, 314-321.

Kokkotou, E., Jeon, J.Y., Wang, X., Marino, F.E., Carlson, M., Trombly, D.J., and Maratos-Flier, E. (2005). Mice with MCH ablation resist diet-induced obesity through strain-specific mechanisms. *Am J Physiol Regul Integr Comp Physiol* 289, R117-124.

Lee, C., Etchegaray, J.P., Cagampang, F.R., Loudon, A.S., and Reppert, S.M. (2001). Posttranslational mechanisms regulate the mammalian circadian clock. *Cell* 107, 855-867.

Selby, C.P., Thompson, C., Schmitz, T.M., Van Gelder, R.N., and Sancar, A. (2000). Functional redundancy of cryptochromes and classical photoreceptors for nonvisual ocular photoreception in mice. *Proceedings of the National Academy of Sciences of the United States of America* 97, 14697-14702.

Zheng, B., Albrecht, U., Kasik, K., Sage, M., Lu, W., Vaishnav, S., Li, Q., Sun, Z.S., Eichele, G., Bradley, A., and Lee, C.C. (2001). Nonredundant roles of the *mPer1* and *mPer2* genes in the mammalian circadian clock. *Cell* 105, 683-694.